Solar Energy Materials and Solar Cells 186 (2018) 194–199

Contents lists available at ScienceDirect

Solar Energy Materials and Solar Cells

journal homepage: www.elsevier.com/locate/solmat

Reassessment of intrinsic lifetime limit in *n*-type crystalline silicon and implication on maximum solar cell efficiency

Boris A. Veith-Wolf[a,*], Sören Schäfer[a], Rolf Brendel[a,b], Jan Schmidt[a,b]

[a] Institute for Solar Energy Research Hamelin (ISFH), Am Ohrberg 1, 31860 Emmerthal, Germany
[b] Institute of Solid-State Physics, Leibniz Universität Hannover, Appelstrasse 2, 30167 Hannover, Germany

ARTICLE INFO

Keywords:
Silicon
Charge carrier lifetime
Intrinsic lifetime
Auger recombination
Surface passivation
Aluminum oxide

ABSTRACT

Unusually high carrier lifetimes are measured by photoconductance decay on *n*-type Czochralski-grown silicon wafers of different doping concentrations, passivated using plasma-assisted atomic-layer-deposited aluminum oxide (Al_2O_3) on both wafer surfaces. The measured effective lifetimes significantly exceed the intrinsic lifetime limit previously reported in the literature. Several prerequisites have to be fulfilled to allow the measurement of such high lifetimes on Al_2O_3-passivated *n*-type silicon wafers: (i) large-area wafers are required to minimize the impact of edge recombination via the Al_2O_3-charge-induced inversion layer, (ii) an exceptionally homogeneous Al_2O_3 surface passivation is required, and (iii) very thick silicon wafers are needed. Based on our lifetime measurements on *n*-type silicon wafers of different doping concentrations, we introduce a new parameterization of the intrinsic lifetime for *n*-type crystalline silicon. This new parameterization has implications concerning the maximum reachable efficiency of *n*-type silicon solar cells, which is larger than assumed before.

1. Introduction

The intrinsic carrier recombination in the crystalline silicon (c-Si) bulk is one of the limiting factors for the maximal achievable energy conversion efficiency of c-Si solar cells. Hence, the exact knowledge of the intrinsic recombination lifetime is of fundamental importance. The intrinsic recombination can be subdivided into radiative and Auger recombination. The Auger recombination cannot be measured directly, in contrast to the radiative recombination [1,2], and is hence up to now a topic of intense research. In the past, the most widely used parameterization of the intrinsic lifetime as a function of doping and excess carrier concentrations was published by Kerr et al. [3]. However, with the later improvements in the surface passivation quality, especially the introduction of the excellent aluminum oxide (Al_2O_3) passivation, a new parameterization was developed by Richter et al. [4]. This parameterization is nowadays the most widespread used intrinsic lifetime parameterization. The parameterization proposed by Richter et al. [4] was derived from lifetime measurements on *n*- and *p*-type silicon samples passivated with Al_2O_3 of various sample sizes. However, as we have shown recently [5], the sample size has a significant impact on the measured lifetime on *n*-type silicon samples passivated with Al_2O_3. In addition to the sample size, the measured lifetime is also affected by the homogeneity of the Al_2O_3 passivation: in particular scratches were shown to have a detrimental impact on the overall lifetime [6]. The reason is the coupling of highly recombination-active sites, such as the sample edges or scratches, via the inversion layer induced by the negative fixed charges within the Al_2O_3 to the measurement area. Hence, the parameterization of Richter et al. [4] is not the uppermost lifetime limit in *n*-type silicon materials, which is supported by a couple of recent publications [6–10]. In our recent study [6], we measured effective lifetimes on 1.4-Ωcm *n*-type silicon wafers significantly exceeding the intrinsic lifetime limit by Richter et al. [4]. In this contribution, we measure the effective lifetime on *n*-type silicon wafers of different resistivities, ranging from 0.87 Ωcm to 3000 Ωcm and derive a new intrinsic lifetime parameterization. We also discuss the impact of our new parameterization on the ultimate efficiency limit for *n*-type c-Si solar cells.

2. Experimental details

We use 6″ and 4″ *n*-type Czochralski-grown silicon (Cz-Si) wafers with different phosphorus doping concentrations, ranging from $\sim 1 \times 10^{12}$ cm^{-3} to 5.8×10^{15} cm^{-3}. The wafers are (100)-oriented and are relatively thick (500–670 µm), which reduces the impact of surface recombination on the measured effective lifetime. The samples are processed as round 6″ or 4″ wafers and only some samples are laser cut into 12.5 × 12.5 cm^2 pseudo-square samples. The latter samples are described in more detail in Ref. 6. In order to clean the wafer bulk from

* Corresponding author.
E-mail address: b.veith-wolf@isfh.de (B.A. Veith-Wolf).

https://doi.org/10.1016/j.solmat.2018.06.029
Received 12 March 2018; Received in revised form 25 May 2018; Accepted 14 June 2018

potential remaining metallic contaminations, selected samples were subject to an impurity gettering step. These samples received a phosphorus diffusion, using $POCl_3$, on both wafer surfaces in a quartz-tube furnace at a temperature of 850 °C resulting in a sheet resistance of (50 ± 4) Ω/sq. The samples are subsequently etched in KOH for 2 min, in order to remove the phosphorus-diffused region at the sample surface. All samples are chemically cleaned using a standard Radio Corporation of America (RCA) cleaning sequence [11]. The samples are symmetrically passivated by 15 nm thick Al_2O_3 layers deposited using plasma-assisted atomic layer deposition (FlexAL™, Oxford Instruments) at a temperature of 200 °C using Trimethylaluminium (TMAl) and an oxygen plasma. The samples are subsequently annealed at 425 °C for 15 min in order to activate the Al_2O_3 passivation. Effective carrier lifetimes τ_{eff} are measured using the photoconductance decay (PCD) method in the transient mode (Sinton Instruments, WCT120 lifetime tester) and the photoconductance-calibrated photoluminescence lifetime imaging (PC-PLI) method [12]. During the lifetime measurements, the sample temperature is measured to be in the range of (302.6 ± 3) K. For the evaluation of the measured data, we assume that the excess carrier concentration is homogeneous over the wafer thickness. This assumption holds true since the bulk diffusion length is much larger than the wafer thickness for all examined samples. The wafer thicknesses are measured using a dial indicator. The doping concentrations n_0 are extracted from the WCT-120 measurements using the mobility model implemented in the data analysis sheet of the lifetime tester. This method cannot be used for the almost undoped samples with a phosphorus doping concentration of $\sim 1 \times 10^{12}$ cm^{-3}. For these samples we assume the doping to be $n_0 = 1 \times 10^{12}$ cm^{-3} (resistivity $\rho = 3000$ Ωcm).

3. Experimental results

The lifetime images measured by PC-PLI show that the passivation quality is extremely homogenous, as can be seen in Fig. 1. Importantly, the measured lifetimes of the *n*-type Cz-Si wafers with doping concentrations $n_0 \geq 3.2 \times 10^{15}$ cm^{-3} significantly exceed the previous intrinsic lifetime parameterization by Richter et al. [4]. In Fig. 2, exemplary injection-dependent lifetime curves are shown for four different doping concentrations. Note that the four shown samples are exemplary samples of each doping concentration. For each doping concentration we have measured a comparable lifetime on at least one more wafer. Table 1 compiles details of all the measured samples. We are able to measure such high effective lifetimes due to the use of large-area (6″ and 4″) samples with a thickness > 500 µm and an excellent homogeneity of the Al_2O_3 surface passivation quality. Note that the lifetimes measured on the lowly doped 3000-Ω cm c-Si sample are well below the Richter parameterization, even at very high injection densities $\Delta n > 5 \times 10^{15}$ cm^{-3}, where Auger recombination fully dominates the measured effective lifetime. Our measurements hence suggest that in the previous Richter parameterization, the lifetimes in *n*-type c-Si have been *underestimated* for doping concentrations exceeding 3×10^{15} cm^{-3} and *overestimated* for low doping levels at high injection densities. Hence, an improved parameterization of the intrinsic lifetime in *n*-type c-Si is required.

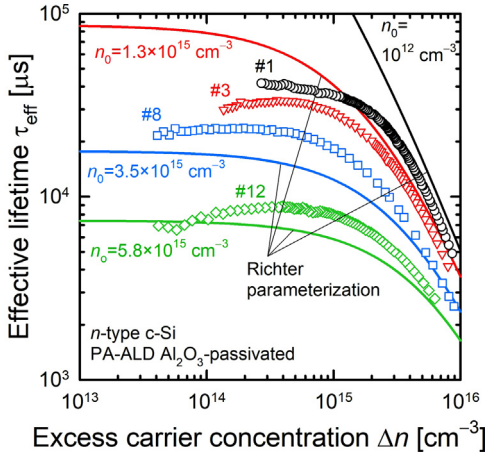

Fig. 2. Effective lifetime τ_{eff} measured using PCD as a function of excess carrier concentration Δn of *n*-type Cz-Si samples with doping concentrations of 1×10^{12} (sample #1, black circles), 1.3×10^{15} (sample #3, red triangles downwards), 3.5×10^{15} cm^{-3} (sample #8, blue squares), and 5.8×10^{15} cm^{-3} (sample #12, green diamonds) passivated with 15 nm Al_2O_3 on both surfaces. Also shown is the intrinsic lifetime parameterization by Richter et al. [4] (lines) (For interpretation of the references to color in this figure, the reader is referred to the web version of this article).

4. New parameterization of the intrinsic lifetime of *n*-type c-Si

Following the approach of Richter et al. [4], we use as a starting point for the intrinsic lifetime of *n*-type crystalline silicon $\tau_{intr.n}$ the equation

$$\tau_{intr.n} = \frac{\Delta n}{(np - n_{i.eff}^2)(g_{eeh}(n_0)\cdot C_n \cdot n_o + g_{\Delta n}(\Delta n)\cdot C_a \cdot \Delta n + B_{rel}B_{low})}, \quad (1)$$

with C_n being the Auger coefficient of the electron-electron-hole process, C_a being the ambipolar Auger coefficient and $B_{low} = 4.76 \times 10^{-15}$ cm^3/s being the radiative recombination coefficient at 300 K, calculated using the generalized Planck law [13] with the absorption coefficient α_{bb}(E) of Green et al. [14], and B_{rel} being the relative radiative recombination coefficient according to Altermatt et al. [2]. We use $C_n = 2.8 \times 10^{-31}$ cm^6/s as measured by Dziewior and Schmid [15]. The enhancement factors $g_{eeh}(n_0)$ and $g_{\Delta n}(\Delta n)$ account for

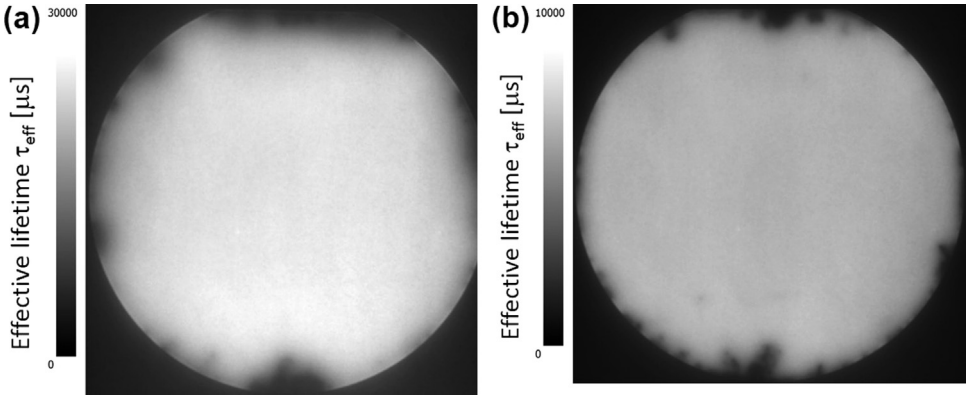

Fig. 1. Photoluminescence lifetime images of *n*-type Cz-Si wafers with doping concentrations of (a) 1.3×10^{15} cm^{-3} (resistivity $\rho = 3.6\,\Omega$ cm) and (b) 5.8×10^{15} cm^{-3} ($\rho = 0.87\,\Omega$ cm). The average excess carrier concentrations are (a) $\Delta n_{av} = 1.2 \times 10^{15}$ cm^{-3} and (b) $\Delta n_{av} = 9.2 \times 10^{14}$ cm^{-3}.

Table 1
Details of the Al_2O_3-passivated *n*-type Cz-Si samples examined in this study. The given lifetimes were measured using the PCD method.

Sample	Resistivity ρ [Ω cm]	Doping concentration n_0 [cm^{-3}]	Wafer thickness W [μm]	Wafer size	Maximum $\tau_{eff.max}$ [ms]	Δn at $\tau_{eff.max}$ [cm^{-3}]	τ_{eff} at $\Delta n = 6 \times 10^{15}$ cm^{-3} [ms]
#1	3000	1×10^{12}	521	4″	41.3	4×10^{14}	8.9
#2	3000	1×10^{12}	510	4″	33.2	2.6×10^{14}	8.5
#3	3.6	1.3×10^{15}	663	6″	33.6	4×10^{14}	6.3
#4	3.6	1.3×10^{15}	660	6″	31.1	2.6×10^{14}	6.1
#5	3.1	1.5×10^{15}	668	6″	28.1	5×10^{15}	6.1
#6	1.5	3.1×10^{15}	600	6″	18.5	6.6×10^{14}	4.6
#7	1.5	3.2×10^{15}	598	6″	21.4	2.3×10^{14}	4.5
#8	1.4	3.5×10^{15}	590	12.5 × 12.5 cm^2	23.7	1.9×10^{14}	4.3
#9	1.3	3.9×10^{15}	600	12.5 × 12.5 cm^2	20.9	1.5×10^{14}	4.1
#10	0.92	5.4×10^{15}	624	6″	9.86	1.6×10^{14}	3.0
#11	0.9	5.6×10^{15}	620	6″	9.23	4.1×10^{14}	3.0
#12	0.87	5.8×10^{15}	618	6″	8.91	4×10^{14}	2.9

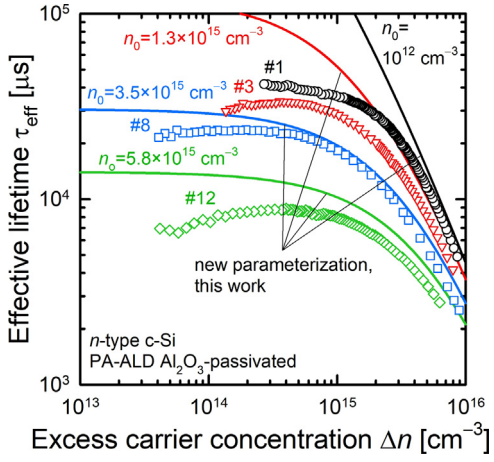

Fig. 3. Effective lifetime τ_{eff} measured using PCD as a function of excess carrier concentration Δn of *n*-type Cz-Si samples with doping concentrations of 1×10^{12} (sample #1, black circles), 1.3×10^{15} (sample #3, red triangles downwards), 3.5×10^{15} (sample #8, blue squares), and 5.8×10^{15} cm^{-3} (sample #12, green diamonds) passivated with 15 nm Al_2O_3 on both surfaces. Also shown is the intrinsic lifetime parameterization according to Eq. (2) (lines) (For interpretation of the references to color in this figure, the reader is referred to the web version of this article).

the Coulomb enhancement of the Auger recombination. For a detailed discussion of the Coulomb enhancement effect, see Ref. 4. For $g_{eeh}(n_0)$ we use Eq. (19) of Ref. 4 and only vary the pre-factor (see Eq. (4) below). We further simplify the equation by neglecting $n_{i.eff}^2$, since $np > > n_{i.eff}^2$ in most practical cases.

In order to approach the actual bulk lifetime as close as possible, the knowledge of the surface recombination velocity (SRV) S_{eff} is required. However, since the passivation of *n*-type silicon with Al_2O_3 leads to extremely low SRVs, which are very difficult to determine experimentally, instead we use [16]

$$S_{eff} = \frac{J_{0s}(N_{dop}+\Delta n)}{q n_i^2}, \tag{2}$$

with J_{0s} being the surface saturation current density and q the elementary charge. We choose $J_{0s} = 0.6$ fA/cm^2 with $n_i = 8.6 \times 10^9$ cm^{-3}, which leads to an S_{eff} value of 0.76 cm/s for $N_{dop} + \Delta n = 1.5 \times 10^{16}$ cm^{-3}, which is within the measurement uncertainty of the S_{eff} of 0.8 cm/s as had been measured on PA-ALD Al_2O_3-passivated c-Si wafers in a thickness variation experiment [4]. We further assume the measurement uncertainty of 20% as discussed in Ref. 4. For the fit of the injection dependence for $\Delta n > 10^{16}$ cm^{-3} we use the lifetime data of sample #2 from Richter et al. [4] and apply the same correction as outlined above. Simulations using Sentaurus Device with the model described in Ref. 5 show that even if assuming completely negligible surface recombination, the lifetime below $\Delta n = 10^{15}$ cm^{-3} is reduced due to coupling of the edge recombination via the Al_2O_3-induced inversion channel to the measurement area. Therefore, only measured lifetimes at injection densities $\Delta n > 10^{15}$ cm^{-3} are taken into account.

The assumed S_{eff} changes the extracted bulk lifetime for most of the samples by maximal 9.6–16.7%, depending on sample type and thickness. Only for sample #2 from Richter et al. [4] the lifetime changes by 42.5% in the relevant injection range. The reason for this large deviation is the fact that this wafer was only 203 μm thick. The impact of S_{eff} on the extracted lifetime of the very thick wafers used in this study lies hence within the measurement uncertainty range. Using a least-square fit to the measured data, the following parameterization for *n*-type c-Si at 300 K is obtained (fit parameters are marked in bold in Eqs. (3) and (4), $\tau_{intr.n}$ in seconds and concentrations in cm^{-3}):

$$\tau_{intr.n} = \frac{\Delta n}{np(g_{eeh}(n_0)2.8 \times 10^{-31} n_0 + \mathbf{2.38 \times 10^{-29}} \Delta n^{\mathbf{0.93}} + B_{rel} B_{low})}, \tag{3}$$

$$g_{eeh}(n_0) = 1 + \mathbf{4.2}\left(1 - \tanh\left(\left(\frac{n_0}{3.3 \times 10^{17}}\right)^{0.66}\right)\right). \tag{4}$$

This new parameterization is based on our lifetime measurements on *n*-type c-Si wafers with doping concentrations $n_0 < 6 \times 10^{15}$ cm^{-3} and the measurements by Dziewior and Schmid [15] on highly doped *n*-type c-Si ($n_0 > 6 \times 10^{18}$ cm^{-3}). In between these doping ranges is the Mott transition of the Coulomb enhancement. Assuming that the Mott transition is well described by the Coulomb enhancement factor given by Richter et al. [4], our new parameterization is valid for arbitrary doping concentrations.

Fig. 3 shows the intrinsic lifetime (solid lines) calculated using this new parameterization in comparison to the measured data. The measured data deviates from the intrinsic lifetime especially below $\Delta n = 10^{15}$ cm^{-3}, as expected from our Sentaurus Device simulations. In Fig. 4(a), the deviation of the measured effective lifetimes and in (b) the deviation of the bulk lifetimes (S_{eff}-corrected effective lifetimes) from the new parameterization are shown. In order to gain access to low injection levels, a passivation scheme would be necessary that does not induce an inversion layer on the *n*-type c-Si surface, such as silicon nitride (SiN_x) [7] or polycrystalline silicon on oxide (POLO) [17]. Fig. 5 shows a direct comparison between our new parameterization with the previous parameterization of Richter et al. [4] in low injection together with some recently published measurement data of other groups showing measured lifetimes exceeding the Richter limit. Our new parameterization results in a slightly lower lifetime compared to the Richter parameterization for low doping concentrations in high injection. For the high-resistivity c-Si wafer with $n_0 = 10^{12}$ cm^{-3}, our new parameterization results at $\Delta n = 10^{16}$ cm^{-3} in a lifetime of 4.52 ms in comparison to 5.06 ms using the Richter parameterization. However,

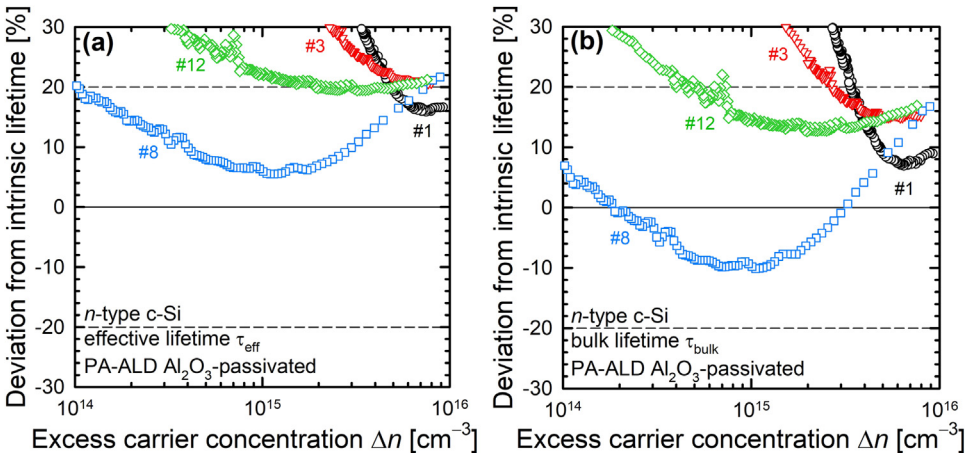

Fig. 4. (a) Deviation of the measured effective lifetimes τ_{eff} and (b) bulk lifetimes τ_{bulk} (S_{eff}-corrected effective lifetimes) from the new intrinsic lifetime parameterization according to Eq. (2) as a function of excess carrier concentration Δn of *n*-type Cz-Si samples with doping concentrations of 1×10^{12} (sample #1, black circles), 1.3×10^{15} (sample #3, red triangles downwards), 3.5×10^{15} (sample #8, blue squares), and 5.8×10^{15} cm^{-3} (sample #12, green diamonds) passivated with 15 nm Al_2O_3 on both surfaces (For interpretation of the references to color in this figure, the reader is referred to the web version of this article).

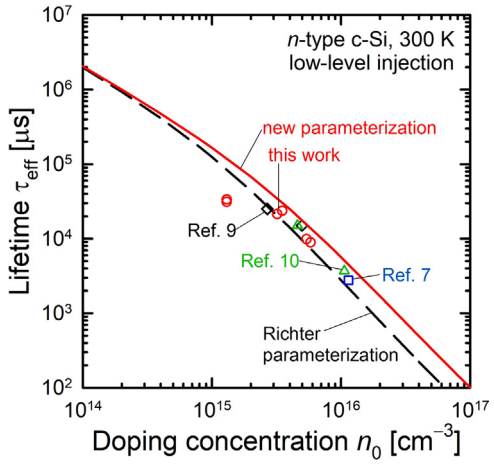

Fig. 5. New intrinsic lifetime parameterization of this study according to Eq. (2) (red line), in comparison with the previous intrinsic lifetime parameterization by Richter et al. [4] (black dashed line) at low-level injection ($\Delta n = 10^{11}$ cm^{-3}). Also shown are maximum measured effective lifetimes reported in this work (red circles) together with published lifetime data of other groups [7,9,10] showing lifetimes exceeding the Richter limit (For interpretation of the references to color in this figure, the reader is referred to the web version of this article).

the difference between both parameterizations is below 20% over the entire injection range. This result is fully consistent with the experimental data of Richter et al. [4], since in Ref. 4 the measured effective lifetimes of the lowly doped c-Si wafers were more than 20% below the proposed parameterization. Hence, it seems consistent that the Richter parameterization slightly overestimates the lifetime in lowly doped and very highly injected silicon. Note that towards low injection, our new parameterization approaches the Richter parameterization, and we calculate at $\Delta n = 10^{14}$ cm^{-3} a lifetime of 2.00 s for our new parameterization and 2.02 s using the Richter parameterization.

5. Impact on limiting efficiency of *n*-type c-Si solar cells

As the intrinsic recombination in the c-Si bulk is one of the limiting factors for the maximal achievable efficiency, our new parameterization of the intrinsic lifetime also changes the fundamental efficiency limit. Richter et al. [18] presented the most recent calculation of the efficiency limit of c-Si solar cells under standard testing conditions [19]. We use their approach, however including the corrected description of the Lambertian light-trapping, as most recently introduced by Schäfer et al. [20], in order to calculate the efficiency limit implied by our new parameterization $\tau_{intr.n}$ given by Eqs. (3) and (4). In order to calculate the fundamental efficiency limit, an ideal solar cell without surface and defect recombination, a perfect front-side antireflection coating, and a perfect rear-side reflection are assumed [18]. For such an ideal solar cell, the current density–voltage (*J*–*V*) characteristic is expressed by [18]

$$J = J_L - qWU_{intr}(V), \tag{5}$$

with J_L being the photo-generated current density, $U_{intr}(V)$ the intrinsic recombination rate and W the cell thickness. In order to calculate the Lambertian light-trapping we use the exact expression, Eq. (2) of Ref. 20, together with the assumption that each absorbed photon creates only one electron-hole pair. For the calculation of J_L we use Eq. (3) of Ref. 18. For the calculation of the dependence of U_{intr} on V the assumption of ideal contacts and a narrow base is made, and hence, Δn is related to V by [18,21]

$$(n_0+\Delta n)(p_0+\Delta n) = n_{i,eff}^2 \quad \exp\left(\frac{qV}{kT}\right), \tag{6}$$

with k being the Boltzmann constant and T the temperature. This equation can be transformed into

$$\Delta n = -\frac{n_0 + p_0}{2} + \sqrt{n_{i,eff}^2 \exp\left(\frac{qV}{kT}\right) + \left(\frac{n_0 + p_0}{2}\right)^2 - n_0 p_0}\,. \tag{7}$$

$n_{i,eff}$ is calculated using Eq. (1) of Ref. 22 with the energy band-gap narrowing calculated using the random-phase approximation model by Schenk [23]. For n_i we use a value of 8.28×10^9 cm^{-3}, as was also used by Richter et al. [18]. The intrinsic recombination is calculated with the intrinsic lifetime according to Eq. (3) including photon recycling, as described in Ref. 20. Finally, the efficiency was calculated numerically by varying V and solving Eq. (5) iteratively. The maximum power was calculated from the maximum value for *JV*. We calculate the efficiency limit from the maximum power. The solar cell thickness is varied in order to find the optimum thickness for each doping concentration.

Fig. 6 shows the efficiency limit of *n*-type silicon solar cells as a function of the doping concentration. Note that the optimum solar cell thickness for each doping concentration was used to calculate the efficiency limit. Our novel parameterization of $\tau_{intr.n}$ in combination with the corrected optical model [20] results in a maximum efficiency of 29.47%, whereas using the previous intrinsic lifetime parameterization of Richter et al. plus their optical model [18] resulted in a maximum efficiency of 29.43%. The accurate description of the Lambertian light-trapping leads to an increase of the efficiency, which is partly compensated by a slightly reduced intrinsic lifetime at the injection density corresponding to the maximum power point Δn_{mpp} of 6.84×10^{15} cm^{-3}. Overall, our new lifetime parameterization plus the more accurate expression of the Lambertian light-trapping lead to an increased efficiency limit for *n*-type silicon solar cells. For a typical 1.5-Ω cm *n*-type silicon wafer with $n_0 = 3 \times 10^{15}$ cm^{-3}, our new parameterization

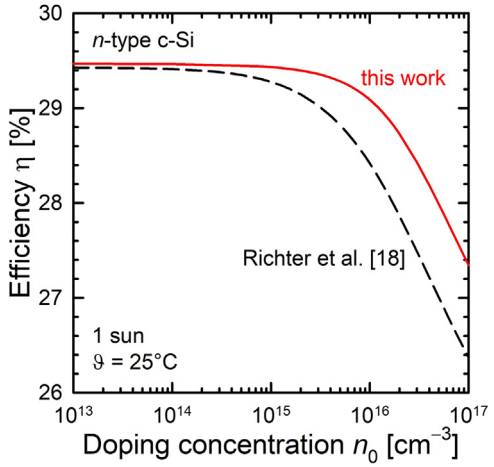

Fig. 6. Efficiency limit η as a function of the doping concentration n_0 for *n*-type silicon solar cells. Shown is the efficiency calculated with the modeling parameters used by Richter et al. [18] (black dashed line) and with our new parameterization according to Eq. (3) plus the improved optical model [20] (red line) (For interpretation of the references to color in this figure, the reader is referred to the web version of this article).

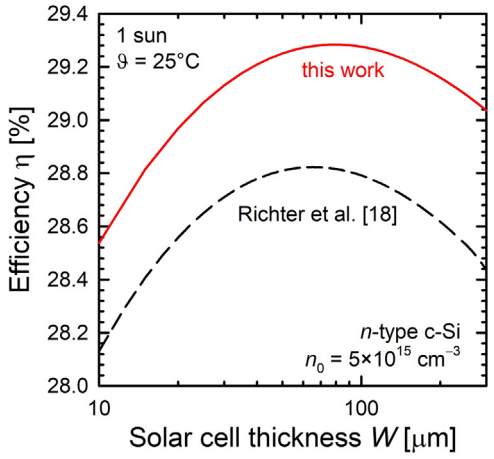

Fig. 7. Efficiency limit η as a function of the solar cell thickness *W* for 1-Ωcm *n*-type silicon solar cells with $n_0 = 5 \times 10^{15}$ cm^{-3}. Shown are the efficiencies calculated using the modeling parameters by Richter et al. [18] (black dashed line) and using our new parameterization according to Eq. (3) including the improved optical model [20] (red line) (For interpretation of the references to color in this figure, the reader is referred to the web version of this article).

plus the improved optical model results in an efficiency limit of 29.36%, whereas using the modeling of Richter et al. [18] resulted in 29.03%. Note that since ours as well as Richter's parameterizations of the intrinsic lifetime are based on experimental data, they have both prone to uncertainties. If we assume a maximum uncertainty of 10% for our new parameterization, we calculate only a corresponding uncertainty of 0.3% (relative) in the calculated efficiency. Hence, the accuracy of the calculated efficiency limits have an estimated maximum uncertainty of only ± 0.1% absolute.

Fig. 7 shows the efficiency limit of 1-Ω cm *n*-type silicon solar cells with $n_0 = 5 \times 10^{15}$ cm^{-3} as a function of the solar cell thickness. Using our new $\tau_{intr.n}$ parameterization together with the improved optical model of Schäfer et al. [20] results in a maximal efficiency of 29.28%, whereas applying the modeling parameters used by Richter et al. [18] results in a limiting efficiency of only 28.82%. The main differences are an increased fill factor *FF* and J_{sc} for the solar cell calculated using our new $\tau_{intr.n}$. The increased *FF* can be attributed to a higher lifetime at the injection density corresponding to the maximum power point Δn_{mpp} of 5×10^{15} cm^{-3}. The increased J_{sc} can be attributed mainly to the improved optical model. In addition, the optimum cell thickness increases from 65 μm for the Richter limit to 80 μm for our new parameterization, and hence, also J_{sc} is increased further.

6. Summary

We have measured lifetimes on *n*-type c-Si wafers that exceed the state-of-the-art intrinsic lifetime parameterization. We were able to measure such high lifetimes by applying an exceptionally homogenous Al_2O_3 surface passivation on thick and large-area silicon wafers. Based on our injection-dependent lifetime measurements on *n*-type c-Si wafers of various resistivities, we have derived a new parameterization of the intrinsic lifetime of *n*-type c-Si. Our new parameterization leads to increased lifetimes for doping concentrations above $n_0 = 2 \times 10^{13}$ cm^{-3} (corresponding to resistivities ρ < 220 Ωcm) and to slightly reduced lifetimes for lowly doped *n*-type c-Si at high injection densities in comparison to the previous parameterization of Richter et al. [4]. The new lifetime parameterization has a direct impact on the maximum achievable efficiency of *n*-type c-Si solar cells. Our calculations including our new parameterization and an improved optical model show that the maximum achievable efficiency is slightly increased from 29.43% to 29.47% for lowly doped silicon. For doping concentrations $n_0 > 8 \times 10^{14}$ cm^{-3} the efficiency is strongly increased compared to the Richter limit. For solar cells on 1-Ωcm *n*-type c-Si ($n_0 = 5 \times 10^{15}$ cm^{-3}), the efficiency limit is increased by 0.46% absolute from 28.82% to 29.28% in comparison to the previous intrinsic lifetime parameterization and the optimum cell thickness is increased from 65 to 80 μm.

Acknowledgment

The authors thank Cornelia Marquardt for the preparation of the samples. This work was funded by the German State of Lower Saxony and the German Federal Ministry of Economics and Energy within the research project “LIMES” (contract no. 0324204D).

References

[1] T. Trupke, M.A. Green, P. Würfel, P.P. Altermatt, A. Wang, J. Zhao, R. Corkish, Temperature dependence of the radiative recombination coefficient of intrinsic crystalline silicon, J. Appl. Phys. 94 (2003) 4930.
[2] P. P. Altermatt, T. Trupke, A. Neisser, Injection dependence of spontaneous radiative recombination in c-Si: experiment, theoretical analysis, and simulation, In: Proceedings of the 5th International Conference on Numerical Simulation of Optoelectronic Devices, Berlin, Germany, 2005, pp. 47–48.
[3] M.J. Kerr, A. Cuevas, General parameterization of Auger recombination in crystalline silicon, J. Appl. Phys. 91 (2002) 2473.
[4] A. Richter, S.W. Glunz, F. Werner, J. Schmidt, A. Cuevas, Improved quantitative description of Auger recombination in crystalline silicon, Phys. Rev. B 86 (2012) 165202.
[5] B. Veith, T. Ohrdes, F. Werner, R. Brendel, P.P. Altermatt, N.-P. Harder, J. Schmidt, Injection dependence of the effective lifetime of *n*-type Si passivated by Al_2O_3: an edge effect? Sol. Energy Mater. Sol. Cells 120 (2014) 436–440.
[6] B. Veith-Wolf, J. Schmidt, Unexpectedly high minority-carrier lifetimes exceeding 20 ms measured on 1.4-Ω cm *n*-type silicon wafers, Phys. Status Solidi RRL 11 (2017) 1700235.
[7] Y. Wan, K.R. McIntosh, A.F. Thomson, A. Cuevas, Low surface recombination velocity by low-absorption silicon nitride on c-si, IEEE J. Photovolt. 3 (2013) 554–559.
[8] T. Niewelt, W.M. Kwapil, M. Selinger, A. Richter, M.C. Schubert, Long-term stability of aluminum oxide based surface passivation schemes under illumination at elevated temperatures, IEEE J. Photovolt. 7 (2017) 1197–1202.
[9] T. Niewelt, A. Richter, T.C. Kho, N.E. Grant, R.S. Bonilla, B. Steinhauser, J.-I. Polzin, F. Feldmann, M. Hermle, J.D. Murphy, S.P. Phang, W. Kwapil, M.C. Schubert, Taking monocrystalline silicon to the ultimate lifetime limit, Sol. Energy Materials Sol. Cells 185 (2018) 252–259.
[10] T. Kho, K. Fong, K.R. McIntosh, E. Franklin, N.E. Grant, M. Stocks, S.P. Phang, Y. Wan, E.-C. Wang, K. Vora, Z. Ngwe, A. Blakers, Exceptional silicon surface passivation by an ONO dielectric stack, Sol. Energy Materials Sol. Cells, submitted.
[11] W. Kern, The evolution of silicon wafer cleaning technology, J. Electrochem. Soc. 137 (1990) 1887–1892.
[12] S. Herlufsen, J. Schmidt, D. Hinken, K. Bothe, R. Brendel, Photoconductance-calibrated photoluminescence lifetime imaging of crystalline silicon, Phys. Status Solidi

RRL 2 (2008) 245–247.
[13] P. Würfel, The chemical potential of radiation, J. Phys. C: Solid State Phys. 15 (1982) 3967.
[14] M.A. Green, Self-consistent optical parameters of intrinsic silicon at 300 K including temperature coefficients, Sol. Energy Mater. Sol. Cells 92 (2008) 1305–1310.
[15] J. Dziewior, W. Schmid, Auger coefficients for highly doped and highly excited silicon, Appl. Phys. Lett. 31 (1977) 346–348.
[16] K.R. McIntosh, L.E. Black, On effective surface recombination parameters, J. Appl. Phys. 116 (2014) 014503.
[17] U. Römer, R. Peibst, T. Ohrdes, B. Lim, J. Krügener, T. Wietler, R. Brendel, Ion implantation for poly-Si passivated back-junction back-contacted solar cells, IEEE J. Photovolt. 5 (2015) 507–514.
[18] A. Richter, M. Hermle, S.W. Glunz, Reassessment of the limiting efficiency for crystalline silicon solar cells, IEEE J. Photovolt. 3 (2013) 1184–1191.
[19] Photovoltaic Devices—Part 3: Measurement Principles for Terrestrial Photovoltaic (PV) Solar Devices With Reference Spectral Irradiance Data, International Standard, IEC 60904–3, 2nd ed., 2008.
[20] S. Schäfer and R. Brendel, Accurate Calculation of the Absorptance Enhances Efficiency Limit of Crystalline Silicon Solar Cells with Lambertian Light Trapping, IEEE J. of Photovoltaics, published online.
[21] M.A. Green, Limits on the open-circuit voltage and efficiency of silicon solar cells imposed by intrinsic auger processes, IEEE Trans. Electron Devices 31 (1984) 671–678.
[22] P.P. Altermatt, A. Schenk, F. Geelhaar, G. Heiser, Reassessment of the intrinsic carrier density in crystalline silicon in view of band-gap narrowing, J. Appl. Phys. 93 (2003) 1598.
[23] A. Schenk, Finite-temperature full random-phase approximation model of band gap narrowing for silicon device simulation, J. Appl. Phys. 84 (1998) 3684–3695.